Structural information about the Ar_6 cluster from the frozen-Gaussian imaginary-time propagator

Holger Cartarius*
Institut für Theoretische Physik 1, Universität Stuttgart, D-70550 Stuttgart, Germany
(Received 4 June 2015; published 24 November 2015)

A numerically cheap way to obtain structural information about clusters of rare gas atoms at low temperatures is developed. The semiclassical frozen-Gaussian imaginary-time propagator is extended such that it can account for the mean values of all interatomic distances in the cluster and their variances. To reduce the required numerical effort an approximation for the mean values is developed which preserves the quality of the results offered by the semiclassical ansatz. The method is applied to the Ar_6 cluster. It is found that the cluster dissociates almost in one step to six free atoms when the temperature is increased. Precursors of the dissociation are only observable in the distances of the atoms via the appearance of a second isomer. The process is almost classical. However, the method is able to resolve small differences in the temperatures at which the dissociation takes place and in the mean distances of the bound configuration.

DOI: 10.1103/PhysRevA.92.052519 PACS number(s): 36.40.Mr, 32.60.+i, 02.30.−f, 32.80.Fb

I. INTRODUCTION

At very low temperatures of a few Kelvin rare gas atoms may assemble and form clusters due to the van der Waals interaction. It has been found in a variety of numerical studies [1–11] that these clusters exhibit a large number of interesting effects. In particular, structural changes of the systems for an increase or decrease of the temperature provide insight into the behavior and binding mechanisms of the quantum mechanical objects at finite temperatures. Thus, rare gas atomic clusters are a topic of ongoing research. Among the rich variety of their thermodynamic properties are a change from one packing of the atoms to another with increasing energy, or phase transitions from a solidlike behavior to a liquidlike arrangement of the atoms [1–7].

For the weak van der Waals interaction between rare gas atoms the thermal energy corresponding to a few Kelvin already suffices to lead to all impacts mentioned above. Thus, accurate quantum mechanical computations are essential to obtain reliable results. In numerical calculations the Boltzmann operator at inverse temperature β, $K = \exp(-\beta H)$, (due to its form also called imaginary-time propagator) is the most important quantity. Its trace yields the partition function $Z(\beta)$, and the thermal averages of every observable O follow from $\langle O\rangle_\beta = \mathrm{Tr}[K(\beta)O]/Z(\beta)$. However, precise calculations for multidimensional systems are still a challenge for today's numerical possibilities. For example, path-integral Monte Carlo methods have been used to investigate rare gas clusters [12–14]. At low temperatures they become already too expensive for a few dozen atoms, and efficient but sufficiently accurate approximations are required. These approximations have to reproduce quantum effects correctly since they will be of eminent importance at low temperatures. Still many questions are open. For example, Ne_{13} and Ne_{38} [4,6,8,9] might exhibit novel low temperature quantum effects, such as liquidlike zero-temperature structures of Ne_{38} as compared to a solidlike structure predicted from classical mechanics [15].

Semiclassical methods help even with presently available computation capabilities to overcome the numerical drawbacks of numerically exact quantum mechanical algorithms and are still developed and applied in a wide context concerning thermodynamic properties [2–4,6,10,11,16–20]. Important semiclassical approximations are based on the idea of restricting the quantum mechanical wave functions to a Gaussian shape. The Gaussian functions are defined completely by a small number of parameters such as the position of the center, a momentum of the wave packet, and a width matrix. The lowest numerical effort is achieved with a frozen-Gaussian propagator, i.e., a Gaussian wave function of which the width matrix in the exponent is fixed for all imaginary times (or temperatures).

Small argon clusters are among those rare gas clusters which attracted large interest for a long time and again recently [7,21–33]. Despite their apparent simplicity numerical calculations turned out to be nontrivial, and for the argon trimer even sophisticated path-integral Monte Carlo calculations could not distinguish a complete dissociation from structural changes within a bound system because the numerics suffered strongly from noise [7]. The frozen-Gaussian imaginary-time propagator has proved to provide high quality results. It could solve this question and identify an almost classical dissociation effect [16], which was confirmed [18] with a first-order correction to the semiclassical imaginary-time propagator [34,35].

For the more complicated Ar_6 cluster the specific heat and mean energy do not provide enough information to understand its whole structure. It is important to know which alignment of the atoms is present. A very detailed knowledge of the atomic structure is available via the interparticle distances. To obtain their values it is very common to compute the radial pair correlation function between particles i and j at positions $\boldsymbol{r}_i$ and $\boldsymbol{r}_j$, respectively,

$$\begin{aligned} p_{ij}(r) &= \langle \delta(|\boldsymbol{r}_i - \boldsymbol{r}_j| - r)\rangle_\beta \\ &= \mathrm{Tr}[K(\beta)\delta(|\boldsymbol{r}_i - \boldsymbol{r}_j| - r)]/Z(\beta), \end{aligned} \tag{1}$$

where $\langle\rangle_\beta$ is the thermal average at inverse temperature β and $K(\beta) = e^{-\beta H}$ represents the imaginary-time propagator at the same temperature [3]. This quantity provides information about the distribution of the distances occurring at every temperature.

*holger.cartarius@itp1.uni-stuttgart.de

It is the purpose of this paper to show that the frozen-Gaussian method applied to atomic clusters in Ref. [16] can be used to determine the distances of the atoms in clusters in a numerically cheap and easy way. To do so, an extension to the semiclassical frozen-Gaussian method will be developed. The mean values and the variances of the distances d_{ij} between atoms i and j can directly be accessed and provide a very clear information of how the atoms are arranged in the cluster. Since the distances d_{ij} of the single pairs can be calculated in parallel with the same Monte Carlo sampling all of these values can be obtained with low numerical extra cost. This provides for N atoms $N(N-1)/2$ independent values, whereas in the pair correlation function (1) small differences in the mean distances might be hidden below broad distributions.

The example of the Ar_6 cluster investigated in this article demonstrates the importance of the additional structural information even in this relatively simple system, which does not undergo a structural transformation in the bound state. The mean energy and the specific heat will show that the cluster dissociates with increasing temperature to a system of six free atoms in one step. However, precursors of the dissociation will only be observable in the distances between the atoms, which will indicate a loss of the ground-state configuration at slightly lower temperatures. The variances of the distances will turn out to be very sensitive to the breakdown of the structure.

The further sections of this paper are organized as follows. In Sec. II mean values and variances for interatomic distances with the frozen-Gaussian method are introduced. For comparison the same values are introduced within the more flexible thawed-Gaussian variant. Then the method is applied to the Ar_6 cluster in Sec. III. After a short introduction of the system (Sec. III A), the confining sphere (Sec. III B), and the proper choice of the Gaussian width matrix (Sec. III C) derivatives of the partition function (Sec. III D) and the structural information (Sec. III E) are investigated. A discussion in Sec. IV concludes the paper.

II. THE FROZEN-GAUSSIAN METHOD

A. Propagator

The method is based on a semiclassical approximation of the thermal operator,

$$K(\beta) = e^{-\beta H}, \tag{2}$$

where $\beta = 1/(kT)$ is the inverse temperature. The approximation consists of evaluating $K(\beta)$ by solving the Bloch equation,

$$-\frac{\partial}{\partial\tau}|\boldsymbol{q}_0,\tau\rangle = H|\boldsymbol{q}_0,\tau\rangle, \tag{3}$$

approximately for a frozen-Gaussian coherent state in position space representation,

$$\langle\boldsymbol{x}|\boldsymbol{q}_0(\tau)\rangle = \left(\frac{\det(\boldsymbol{\Gamma})}{\pi^{3N}}\right)^{1/4}\exp\Big(-\frac{1}{2}[\boldsymbol{x}-\boldsymbol{q}(\tau)]^{\mathrm{T}}\boldsymbol{\Gamma}[\boldsymbol{x}-\boldsymbol{q}(\tau)] + \frac{i}{\hbar}\boldsymbol{p}^{\mathrm{T}}(\tau)\cdot[\boldsymbol{x}-\boldsymbol{q}(\tau)]\Big), \tag{4}$$

where the width matrix $\boldsymbol{\Gamma}$ is a free parameter and has to be adapted to the given problem as will be explained later for the cluster considered in this article. The propagation in Eq. (3) is done in imaginary time τ up to the value $\tau = \beta$ one is interested in.

With Gaussian averages of the type

$$\langle h(\boldsymbol{q})\rangle = \int_{-\infty}^{\infty} d\boldsymbol{x}^{3N}\,|\langle\boldsymbol{x}|\boldsymbol{q}_0(\tau)\rangle|^2 h(\boldsymbol{x}) \tag{5}$$

the symmetrized form of the frozen-Gaussian propagator is given by

$$\begin{aligned}\langle\boldsymbol{x}'|K_{\mathrm{FG}}(\tau)|\boldsymbol{x}\rangle &= \det(\boldsymbol{\Gamma})\exp\Big(-\frac{\hbar^2}{4}\mathrm{Tr}(\boldsymbol{\Gamma})\tau\Big)\sqrt{\det[2(\mathbf{1}-\exp(-\hbar^2\boldsymbol{\Gamma}\tau))^{-1}]}\\ &\times\exp\Big(-\frac{1}{4}[\boldsymbol{x}'-\boldsymbol{x}]^{\mathrm{T}}\boldsymbol{\Gamma}[\tanh(\hbar^2\boldsymbol{\Gamma}\tau/2)]^{-1}[\boldsymbol{x}'-\boldsymbol{x}]\Big)\\ &\times\int_{-\infty}^{\infty}\frac{d\boldsymbol{q}^{3N}}{(2\pi)^{3N}}\exp\Big(-2\int_0^{\tau/2}d\tau\,\langle V(\boldsymbol{q}(\tau))\rangle\\ &-[\bar{\boldsymbol{x}}-\boldsymbol{q}(\tau/2)]^{\mathrm{T}}\boldsymbol{\Gamma}[\bar{\boldsymbol{x}}-\boldsymbol{q}(\tau/2)]\Big),\end{aligned} \tag{6}$$

where $\bar{\boldsymbol{x}} = (\boldsymbol{x}'+\boldsymbol{x})/2$. The partition function is simply given by its trace [35],

$$\begin{aligned}Z_{\mathrm{FG}}(\tau) = \mathrm{Tr}[K_{\mathrm{FG}}(\tau)] &= \sqrt{\det(\boldsymbol{\Gamma})}\exp\Big(-\frac{\hbar^2}{4}\mathrm{Tr}(\boldsymbol{\Gamma})\tau\Big)\\ &\times\sqrt{\det[(\mathbf{1}-\exp(-\hbar^2\boldsymbol{\Gamma}\tau))^{-1}]}\\ &\times\int_{-\infty}^{\infty}\frac{d\boldsymbol{q}^{3N}}{(2\pi)^{N/2}}\exp\Big(-2\int_0^{\tau/2}d\tau\,\langle V(\boldsymbol{q}(\tau))\rangle\Big).\end{aligned} \tag{7}$$

The whole dynamical information is contained in the imaginary-time propagation of the variable $\boldsymbol{q}(\tau)$ and is governed by the $3N$ coupled equations of motion,

$$\frac{\partial\boldsymbol{q}(\tau)}{\partial\tau} = -\boldsymbol{\Gamma}^{-1}\langle\nabla V(\boldsymbol{q}(\tau))\rangle, \tag{8}$$

which are relatively simple and can be integrated with a standard integrator for ordinary differential equations. The remaining numerical task is a single position space integration for the initial positions $\boldsymbol{q}(0)$ in Eq. (6) or (7), which is done with a Monte Carlo integration.

As shown previously [16,18] a reasonable choice of the width matrix is crucial for the quality of the semiclassical method. However, highly precise values can be obtained already with a very simple structure. Since all particles are identical and thus the pairwise interactions are the same for all combinations only the center-of-mass motion has to be distinguished. In center-of-mass coordinates,

$$\boldsymbol{R}_{\mathrm{cm}} = \frac{1}{N}\sum_{i=1}^{N}\boldsymbol{r}_i, \tag{9a}$$

$$\boldsymbol{R}_i = \boldsymbol{r}_i - \boldsymbol{r}_{i+1}, \quad i = 1\ldots, \quad N-1, \tag{9b}$$

good semiclassical estimates are obtained with the matrix

$$\mathbf{\Gamma}_{\mathrm{cmc}} = \begin{pmatrix} \boldsymbol{D}_1 & \mathbf{0} & \cdots \\ \mathbf{0} & \boldsymbol{D}_2 & \\ \vdots & & \ddots \end{pmatrix} \tag{10}$$

and the 3×3 diagonal matrices $\boldsymbol{D}_1$ and $\boldsymbol{D}_2$ describing the three spacial directions of the center of mass and the relative coordinates, respectively. Since also the spacial directions are equivalent the best choice are multiples of the unity matrix $\mathbf{1}_{3\times3}$, such that two scalar coefficients D_1 and D_2 have to be chosen, i.e.,

$$\boldsymbol{D}_1 = D_1 \mathbf{1}_{3\times3}, \quad \boldsymbol{D}_2 = D_2 \mathbf{1}_{3\times3}. \tag{11}$$

The form (6) of the propagator is represented in Cartesian coordinates and is the most efficient for the numerical evaluation. Consequently the Cartesian representation,

$$\mathbf{\Gamma} = \begin{pmatrix} \bar{\boldsymbol{D}} & \Delta\boldsymbol{D} & \Delta\boldsymbol{D} & \\ \Delta\boldsymbol{D} & \bar{\boldsymbol{D}} & \Delta\boldsymbol{D} & \cdots \\ & & \ddots & \end{pmatrix}, \tag{12a}$$

$$\bar{\boldsymbol{D}} = (\boldsymbol{D}_1 + (N-1)\boldsymbol{D}_2)/N, \tag{12b}$$

$$\Delta\boldsymbol{D} = (\boldsymbol{D}_1 - \boldsymbol{D}_2)/N \tag{12c}$$

of the matrix (10) is used.

B. Thermal averages of structural information

Simple thermal averages requiring only the partition function $Z(\beta)$ are the mean energy $E = \mathrm{k}T^2 \partial \ln Z/\partial T$ and the specific heat $C = \partial E/\partial T$. However, $K(\beta)$ provides access to the thermal average of any observable O via

$$\bar{O}^{(\mathrm{FG})} = \frac{\mathrm{Tr}[K_{\mathrm{FG}}(\beta) O]}{Z_{\mathrm{FG}}(\beta)}, \tag{13}$$

which is exploited in this article to gain access to the structural information. A well-suited property is the distance between two atoms, i.e.,

$$O = d_{ij} = |\boldsymbol{x}_i - \boldsymbol{x}_j|. \tag{14}$$

With the frozen-Gaussian propagator (6) this leads to the expression

$$\begin{aligned} \bar{d}_{ij}^{(\mathrm{FG})} &= \frac{1}{Z_{\mathrm{FG}}(\beta)} \mathrm{Tr}[K_{\mathrm{FG}}(\beta)\, |\boldsymbol{x}_i - \boldsymbol{x}_j|] \\ &= \frac{1}{Z_{\mathrm{FG}}(\beta)} \det(\mathbf{\Gamma}) \exp\left(-\frac{\hbar^2}{4}\mathrm{Tr}(\mathbf{\Gamma})\beta\right) \\ &\quad \times \sqrt{\det[2(\mathbf{1} - \exp(-\hbar^2\mathbf{\Gamma}\beta))^{-1}]} \\ &\quad \times \int_{-\infty}^{\infty} \frac{d\boldsymbol{q}^{3N}}{(2\pi)^{3N}} \exp\left(-2\int_0^{\beta/2} d\tau \langle V(\boldsymbol{q}(\tau))\rangle\right) \\ &\quad \times \int_{-\infty}^{\infty} d\boldsymbol{x}^{3N} \exp(-[\boldsymbol{x} - \boldsymbol{q}(\beta/2)]^{\mathrm{T}} \\ &\quad \times \mathbf{\Gamma}[\boldsymbol{x} - \boldsymbol{q}(\beta/2)])|\boldsymbol{x}_i - \boldsymbol{x}_j|, \end{aligned} \tag{15}$$

in which an explicit integration over the $3N$ position variables $\boldsymbol{x}$ remains in addition to the evaluation of the partition function (7). As mentioned previously [18] it is very important to reduce the numerical effort as much as possible for many-particle systems. In particular, the position space integrations require an expensive Monte Carlo sampling in a high-dimensional configuration space.

For usual applications a numerical evaluation of the $\boldsymbol{x}$ integration can be avoided in a reasonable approximation. This can be seen with the variable $\boldsymbol{y} = \boldsymbol{x} - \boldsymbol{q}(\beta/2)$, which transforms the $\boldsymbol{x}$ integral in (15) to

$$I = \int_{-\infty}^{\infty} d\boldsymbol{y}^{3N} \exp(-\boldsymbol{y}^{\mathrm{T}}\mathbf{\Gamma}\boldsymbol{y})|\boldsymbol{y}_i - \boldsymbol{y}_j + \boldsymbol{q}_i(\beta/2) - \boldsymbol{q}_j(\beta/2)|. \tag{16}$$

The widths of the atom's wave functions contribute only at low temperatures significantly to the distance. As will be seen, in practical applications a very narrow Gaussian centers all values $\boldsymbol{y}_i$ strongly around zero, i.e., $\boldsymbol{x}_i$ is almost identical with $\boldsymbol{q}_i(\beta/2)$ for a nonvanishing Gaussian weight. Thus, the integral (16) is calculated for the case $|\boldsymbol{y}_i - \boldsymbol{y}_j| \ll |\boldsymbol{q}_i - \boldsymbol{q}_j|$. With the expansion

$$\begin{aligned} &|\boldsymbol{y}_i - \boldsymbol{y}_j + \boldsymbol{q}_i - \boldsymbol{q}_j| \\ &\quad \approx |\boldsymbol{q}_i - \boldsymbol{q}_j| - (\boldsymbol{y}_i - \boldsymbol{y}_j) \cdot \frac{\boldsymbol{q}_i - \boldsymbol{q}_j}{|\boldsymbol{q}_i - \boldsymbol{q}_j|} \\ &\qquad + \frac{1}{2}(\boldsymbol{y}_i - \boldsymbol{y}_j)^2 - \frac{1}{2}\frac{[(\boldsymbol{y}_i - \boldsymbol{y}_j)\cdot(\boldsymbol{q}_i - \boldsymbol{q}_j)]^2}{|\boldsymbol{q}_i - \boldsymbol{q}_j|^3} \end{aligned} \tag{17}$$

the integral evaluates to

$$\begin{aligned} I = \sqrt{\frac{\pi^{3N}}{\det(\mathbf{\Gamma})}} \Bigg[&|\boldsymbol{q}_i(\beta/2) - \boldsymbol{q}_j(\beta/2)| \\ &+ \frac{\mathrm{Tr}\left(\mathbf{\Gamma}_{ii}^{-1} + \mathbf{\Gamma}_{jj}^{-1} - \mathbf{\Gamma}_{ij}^{-1} - \mathbf{\Gamma}_{ji}^{-1}\right)}{6|\boldsymbol{q}_i(\beta/2) - \boldsymbol{q}_j(\beta/2)|} \Bigg], \end{aligned} \tag{18}$$

where $\mathbf{\Gamma}_{ij}$ is the 3×3 submatrix of $\mathbf{\Gamma}$ at the rows and columns representing particles i and j. In total

$$\begin{aligned} \bar{d}_{ij}^{(\mathrm{FG})}(\beta) &= \frac{1}{Z_{\mathrm{FG}}(\beta)} \mathrm{Tr}[K_{\mathrm{FG}}(\beta)\, |\boldsymbol{x}_i - \boldsymbol{x}_j|] \\ &\approx \frac{1}{Z_{\mathrm{FG}}(\beta)} \sqrt{\det(\mathbf{\Gamma})} \exp\left(-\frac{\hbar^2}{4}\mathrm{Tr}(\mathbf{\Gamma})\beta\right) \\ &\quad \times \sqrt{\det[(\mathbf{1} - \exp(-\hbar^2\mathbf{\Gamma}\beta))^{-1}]} \\ &\quad \times \int_{-\infty}^{\infty} \frac{d\boldsymbol{q}^{3N}}{(2\pi)^{3N/2}} \exp\left(-2\int_0^{\beta/2} d\tau \langle V(\boldsymbol{q}(\tau))\rangle\right) \\ &\quad \times \Bigg[|\boldsymbol{q}_i(\beta/2) - \boldsymbol{q}_j(\beta/2)| \\ &\qquad + \frac{\mathrm{Tr}\left(\mathbf{\Gamma}_{ii}^{-1} + \mathbf{\Gamma}_{jj}^{-1} - \mathbf{\Gamma}_{ij}^{-1} - \mathbf{\Gamma}_{ji}^{-1}\right)}{6|\boldsymbol{q}_i(\beta/2) - \boldsymbol{q}_j(\beta/2)|} \Bigg], \end{aligned} \tag{19}$$

is obtained.

The first term in Eq. (19), $\propto |\boldsymbol{q}_i - \boldsymbol{q}_j|$, reflects the core of the semiclassical approximation, in which the positions of the atoms are given by the centers $\boldsymbol{q}_i$ of the Gaussian wave packets (4). It corresponds to

$$O = |\boldsymbol{q}_i - \boldsymbol{q}_j|. \tag{20}$$

The second term contains a correction due to the finite width of an atom's wave packet. It is completely sufficient to include this lowest-order term, of which the $\boldsymbol{x}$ integration could be done analytically with a simple result, thus reducing the numerical effort drastically. For the frozen-Gaussian method any higher terms beyond those included in the approximation (19) for the mean distances are of lower interest. From the physical point of view it is expected that the width of the atom's wave function only plays a role at very low temperatures at which the structural configuration is unambiguously in a highly symmetric ground-state configuration. Indeed, as will be seen in the results already the correction term in the approximation (19) is very small.

To estimate the quality and validity of these mean values additionally the variances of the distance distributions are calculated. With the operator

$$O = v_{ij} = (\boldsymbol{x}_i - \boldsymbol{x}_j)^2 - \bar{d}_{ij}^2 \tag{21}$$

and the integral

$$\begin{aligned}
&\frac{1}{Z_{\mathrm{FG}}(\beta)}\mathrm{Tr}[K_{\mathrm{FG}}(\beta)\,(\boldsymbol{x}_i - \boldsymbol{x}_j)^2] \\
&\quad= \frac{1}{Z_{\mathrm{FG}}(\beta)}\sqrt{\det(\boldsymbol{\Gamma})}\exp\left(-\frac{\hbar^2}{4}\mathrm{Tr}(\boldsymbol{\Gamma})\beta\right) \\
&\qquad\times\sqrt{\det[(\mathbf{1}-\exp(-\hbar^2\boldsymbol{\Gamma}\beta))^{-1}]} \\
&\qquad\times\int_{-\infty}^{\infty}\frac{d\boldsymbol{q}^{3N}}{(2\pi)^{3N/2}}\exp\left(-2\int_0^{\beta/2}d\tau\,\langle V(\boldsymbol{q}(\tau))\rangle\right) \\
&\qquad\times\Bigg[(\boldsymbol{q}_i(\beta/2)-\boldsymbol{q}_j(\beta/2))^2 \\
&\qquad+\frac{1}{2}\mathrm{Tr}\big(\boldsymbol{\Gamma}_{ii}^{-1}+\boldsymbol{\Gamma}_{jj}^{-1}-\boldsymbol{\Gamma}_{ij}^{-1}-\boldsymbol{\Gamma}_{ji}^{-1}\big)\Bigg],
\end{aligned} \tag{22}$$

the standard deviations $\sigma_{ij} = \sqrt{\bar{v}_{ij}^{(\mathrm{FG})}}$ of the distances $\bar{d}_{ij}^{(\mathrm{FG})}$ are obtained.

C. Sorted distances

For the Ar_6 cluster there are 15 possible combinations i and j, and thus 15 distances. The clusters are oriented arbitrarily in the simulation. The numbers i and j of the atoms have no meaning for the true configuration, and thus are not appropriate quantities to define the pairwise distances. The average of all calculations simply results in identical values for all $\bar{d}_{ij}$, which correspond to the mean value of all 15 atom-atom distances in a certain configuration. To obtain a meaningful quantity the distances are sorted according to their size,

$$d_1 < d_2 < \ldots < d_{15}, \tag{23}$$

and the thermal average of these size-ordered distances is determined, i.e., the thermal mean values of the smallest distance, the second smallest, and so forth are obtained. These values can be compared with the expectations of geometrical configurations. In an experiment the single distances are accessible [36] and can in a given sample be sorted the same way. Alternatively, results from this calculation can be used to determine the distance of the atoms with a well-grounded assumption about the configuration [37].

D. Comparison with the thawed-Gaussian propagator

The frozen-Gaussian method has proved to provide good results for thermodynamic quantities. We want to know whether or not this is also true for the widths calculated in this article. Thus, the structural information of the frozen-Gaussian method is compared with that of a more flexible thawed-Gaussian ansatz. It is based on a time-dependent width matrix $\boldsymbol{G}(\tau)$, which adapts itself to the given temperature. With the restriction to Gaussian wave packets the thawed-Gaussian variant is usually the most accurate approximation. The variable width matrix adds an additional freedom in the parameters. This is reflected in the quality of the results as has clearly been demonstrated for a double-well potential [38]. For a large number of degrees of freedom it suffers, however, from the higher numerical costs. The single-particle ansatz of Frantsuzov *et al.* [3] avoids these difficulties by reducing the matrix $\boldsymbol{G}(\tau)$ to a block-diagonal structure, where 3×3 matrices representing the three spacial coordinates of one particle are the only nonvanishing matrix elements. In the case of six atoms this reduction is not required and there is no need to ignore the interparticle correlations.

The thawed-Gaussian propagator used for comparison with the frozen-Gaussian method is the time-evolved Gaussian approximation (TEGA) suggested by Frantsuzov *et al.* [3,39] with a full width matrix $\boldsymbol{G}$. It is based on the solution of the Bloch equation (3) with the coherent state

$$\begin{aligned}
\langle \boldsymbol{x}|g(\boldsymbol{q}(\tau),\boldsymbol{G}(\tau))\rangle = (\pi^{3N}|\det\boldsymbol{G}(\tau)|)^{-1/4}\exp\big(-\tfrac{1}{2}[\boldsymbol{x}-\boldsymbol{q}(\tau)]^{\mathrm{T}} \\
\times\boldsymbol{G}(\tau)^{-1}[\boldsymbol{x}-\boldsymbol{q}(\tau)]\big).
\end{aligned} \tag{24}$$

The resulting symmetrized propagator reads

$$\begin{aligned}
&\langle \boldsymbol{x}|K_{\mathrm{TG}}(\tau)|\boldsymbol{x}'\rangle \\
&\quad= \int\frac{d\boldsymbol{q}^{3N}}{(2\pi)^{3N}}\frac{\exp[2\gamma(\tau/2)]}{\det[\boldsymbol{G}(\tau/2)]} \\
&\qquad\times\exp\left(-\frac{1}{2}[\boldsymbol{x}-\boldsymbol{q}(\tau/2)]^{\mathrm{T}}\boldsymbol{G}(\tau/2)^{-1}[\boldsymbol{x}-\boldsymbol{q}(\tau/2)]\right) \\
&\qquad\times\exp\left(-\frac{1}{2}[\boldsymbol{x}'-\boldsymbol{q}(\tau/2)]^{\mathrm{T}}\boldsymbol{G}(\tau/2)^{-1}[\boldsymbol{x}'-\boldsymbol{q}(\tau/2)]\right),
\end{aligned} \tag{25}$$

with the time-dependent width matrix $\boldsymbol{G}(\tau)$. In imaginary time τ the equations of motion for the Gaussian parameters $\boldsymbol{G}$, $\boldsymbol{q}$, and γ are

$$\frac{d}{d\tau}\boldsymbol{G}(\tau) = -\boldsymbol{G}(\tau)\langle\nabla\nabla^{\mathrm{T}}V(\boldsymbol{q}(\tau))\rangle\boldsymbol{G}(\tau) + \hbar^2\mathbf{1}, \tag{26a}$$

$$\frac{d}{d\tau}\boldsymbol{q}(\tau) = -\boldsymbol{G}(\tau)\langle\nabla V(\boldsymbol{q}(\tau))\rangle, \tag{26b}$$

$$\frac{d}{d\tau}\gamma(\tau) = -\frac{1}{4}\mathrm{Tr}[\langle\nabla\nabla^{\mathrm{T}}V(\boldsymbol{q}(\tau))\rangle\boldsymbol{G}(\tau)] - \langle V(\boldsymbol{q}(\tau))\rangle, \tag{26c}$$

which have to be integrated from $\tau = 0$ to larger times with the initial conditions,

$$\boldsymbol{q}(\tau\approx 0) = \boldsymbol{q}_0, \tag{27a}$$

$$G(\tau\approx 0) = \hbar^2\mathbf{1}\tau, \tag{27b}$$

$$\gamma(\tau\approx 0) = -V(\boldsymbol{q}_0)\tau. \tag{27c}$$

In all expressions $\langle \dots \rangle$ represents Gaussian averaged quantities of the form (5) with the wave packet (24), and $\mathbf{1}$ is the $3N \times 3N$-dimensional identity matrix. The relevant quantities are the partition function,

$$Z_{\mathrm{TG}} = \int \frac{d\boldsymbol{q}^{3N}}{(2\sqrt{\pi})^{3N}} \frac{\exp[2\gamma(\tau/2)]}{\sqrt{\det[\boldsymbol{G}(\tau/2)]}}, \tag{28}$$

and the mean value of the distances in the same approximation as for the frozen-Gaussian method,

$$\bar{d}_{ij}^{(\mathrm{TG})}(\beta) \approx \frac{1}{Z_{\mathrm{TG}}(\beta)} \int \frac{d\boldsymbol{q}^{3N}}{(2\sqrt{\pi})^{3N}} \frac{\exp[2\gamma(\beta/2)]}{\sqrt{\det[\boldsymbol{G}(\beta/2)]}} \left[|\boldsymbol{q}_i(\beta/2) - \boldsymbol{q}_j(\beta/2)| + \frac{\mathrm{Tr}[\boldsymbol{G}_{ii}(\beta/2) + \boldsymbol{G}_{jj}(\beta/2) - \boldsymbol{G}_{ij}(\beta/2) - \boldsymbol{G}_{ji}(\beta/2)]}{6|\boldsymbol{q}_i(\beta/2) - \boldsymbol{q}_j(\beta/2)|} \right]. \tag{29}$$

The thawed-Gaussian approximation allows for an additional important information. Its temperature-dependent width matrix $\boldsymbol{G}(\tau)$ provides easier access to the width of the wave function, which influences the variances of the distances. The quantum mechanical part of the variances, i.e., that originating from the spread of the wave function, is expected to increase at lower temperatures. For a frozen Gaussian this can be described correctly if the constant matrix $\boldsymbol{\Gamma}$ is optimized for every single temperature. In the thawed-Gaussian case the variances read

$$\bar{v}_{ij}^{(\mathrm{TG})}(\beta) \approx \frac{1}{Z_{\mathrm{TG}}(\beta)} \int \frac{d\boldsymbol{q}^{3N}}{(2\sqrt{\pi})^{3N}} \frac{\exp[2\gamma(\beta/2)]}{\sqrt{\det[\boldsymbol{G}(\beta/2)]}} \left[(\boldsymbol{q}_i(\beta/2) - \boldsymbol{q}_j(\beta/2))^2 + \frac{1}{2}\mathrm{Tr}[\boldsymbol{G}_{ii}(\beta/2) + \boldsymbol{G}_{jj}(\beta/2) - \boldsymbol{G}_{ij}(\beta/2) - \boldsymbol{G}_{ji}(\beta/2)] \right] - \left(\bar{d}_{ij}^{(\mathrm{TG})}\right)^2, \tag{30}$$

and follow directly from the imaginary-time evolution of $\boldsymbol{q}(\tau)$ *and* $\boldsymbol{G}(\tau)$. We are mainly interested in the quantum mechanical part of the variances, viz.

$$\bar{v}_{ij}^{(\mathrm{TG,qm})}(\beta) \approx \frac{1}{Z_{\mathrm{TG}}(\beta)} \int \frac{d\boldsymbol{q}^{3N}}{(2\sqrt{\pi})^{3N}} \frac{\exp[2\gamma(\beta/2)]}{\sqrt{\det[\boldsymbol{G}(\beta/2)]}} \frac{1}{2}\mathrm{Tr}[\boldsymbol{G}_{ii}(\beta/2) + \boldsymbol{G}_{jj}(\beta/2) - \boldsymbol{G}_{ij}(\beta/2) - \boldsymbol{G}_{ji}(\beta/2)]. \tag{31}$$

III. STRUCTURAL INFORMATION ABOUT THE Ar_6 CLUSTER

A. Representation of the system

The argon cluster consists of six atoms, where the Hamiltonian in mass scaled coordinates reads

$$H = -\frac{\hbar^2}{2} \sum_{i=1}^{6} \Delta_i + \sum_{j<i} V(r_{ij}), \tag{32}$$

with the Laplacian Δ_i of particle i. The two-body potential $V(r_{ij})$ of argon is still a very challenging task. One of the best analytic expressions at hand is a fit to experimental results by Aziz and Slaman [40] of which an adoption to a Morse potential [25] is used,

$$V(r_{ij}) = D(\exp[-2\alpha(r_{ij} - R_{\mathrm{e}})] - 2\exp[-\alpha(r_{ij} - R_{\mathrm{e}})]), \tag{33}$$

with the parameters $D = 99.00\,\mathrm{cm}^{-1}$, $\alpha = 1.717\,\text{Å}$, and $R_{\mathrm{e}} = 3.757\,\text{Å}$ in consistence with previous studies of the argon trimer [7,16,18].

The numerical efficiency of the frozen-Gaussian method is increased with an expansion of the potential in terms of Gaussians, viz.

$$V(|\boldsymbol{r}_i - \boldsymbol{r}_j|) = \sum_p c_p e^{-\alpha_p r_{ij}^2}, \qquad r_{ij} = |\boldsymbol{r}_i - \boldsymbol{r}_j|. \tag{34}$$

This procedure was suggested by Frantsuzov *et al.* [3] and has successfully been applied [3,16,18]. In the form (34) Gaussian integrals of the potential or its derivatives can be done analytically. The required parameters for a fit to three Gaussians are listed in Table I and were previously obtained in Ref. [16].

B. Confining sphere

An additional potential is usually introduced to converge the numerical $\boldsymbol{q}$ integration. All particles are confined within a sphere around the center of mass $\boldsymbol{R}_{\mathrm{cm}}$ by the condition $|\boldsymbol{q} - \boldsymbol{R}_{\mathrm{cm}}| < R_c$, where R_c is the confining radius. This can be achieved with the steep potential

$$V_{\mathrm{c}}(\boldsymbol{r}) \propto \sum_{i=1}^{N} \left(\frac{\boldsymbol{r}_i - \boldsymbol{R}_{\mathrm{cm}}}{R_{\mathrm{c}}} \right)^{20} \tag{35}$$

added to the Hamiltonian (32) or, as in our study, by a restriction of the volume for the $\boldsymbol{q}$ integration.

Of course, an additional potential influences the results and can crucially change the behavior of the cluster [2,21]. If only bound configurations are investigated R_{c} is usually chosen such that the bound configurations are not affected, i.e., R_{c} is larger than the extension of the bound cluster. However, we are interested also in the dissociation process for which the choice of R_{c} is nontrivial [16,18]. A larger radius R_{c} always allows for a dissociation at lower temperatures. In principle it has to be adopted to the physical conditions as, e.g., the pressure. We are interested in the qualitative behavior at the dissociation and

TABLE I. Parameters of the argon-argon interaction potential expressed in terms of Gaussians according to Eq. (34) [16].

p	c_p (cm^{-1})	α_p (Å^{-2})
1	3.296×10^5	0.6551
2	-1.279×10^3	0.1616
3	-9.946×10^3	6.0600

it was checked carefully that the choice $R_c = 35$ Å does not influence the qualitative change of the relevant observables, i.e., the mean energy, the specific heat, the mean values of the interatomic distances, and their variances. In particular, it was assured that the case of a completely dissociated cluster is present for temperatures above 40 K and the form of the dissociation process is not altered. The value of the confining radius R_c, i.e., the pressure in physical terms, affects the temperature at which the dissociation occurs.

C. Choice of the width matrix

While in a thawed-Gaussian calculation the initial condition for the width matrix (27b) is defined, the constant matrix $\mathbf{\Gamma}$ of its frozen-Gaussian counterpart has to be chosen carefully. It is a free parameter of the system. It is not trivial to find a good choice of $\mathbf{\Gamma}$. However, as was mentioned above, the structure (12) with the 3×3 submatrices (11) is well suited. Thus, only the two parameters D_1 and D_2 need to be chosen.

A detailed investigation of the Ar_3 cluster revealed that there is a reliable and simple method to find the best choice for the interparticle width parameter D_2 [16]. Propagating the partition function (7) to long imaginary times $\beta \to \infty$, i.e., $T \to 0$, one can extract the thermodynamic mean energy to correspond to the ground-state energy E_0. The parameter D_2 providing the lowest value for E_0 has shown to lead to the best agreement with numerically exact calculations and the more flexible thawed-Gaussian approximation. This result is almost independent of the temperature at which the partition function, mean energy or specific heat of all methods are compared. Furthermore, calculating the first-order correction to the frozen-Gaussian propagator (6) showed that this choice also requires the smallest correction. Thus, the simple minimization of the ground-state energy gives us a reliable way of determining D_2. For the Ar_6 cluster in this article it was found that $D_2 = 32\,\text{Å}^{-2}$ is the best choice.

The center of mass is free and it can exactly be described by a Gaussian in the limit $D_1 \to 0$. This means the value should be as small as possible. For the numerical evaluation one needs a finite value. It is known that $D_1 = 0.1\,\text{Å}^{-2}$ is small enough [16]. The results cannot be distinguished from those of even lower values for D_1.

D. Mean energy and specific heat

To compare the Ar_6 cluster with the trimer considered in [16,18] the mean energy and the specific heat are studied first. They are shown in Fig. 1 for the two-parameter (D_1 and D_2) frozen-Gaussian propagator and the derivatives of the classical partition function,

$$Z_{\text{cl}} = \left(\frac{\text{k}T}{2\pi\hbar^2}\right)^{3/2N} \int e^{-\beta V(\boldsymbol{q})}\, d\boldsymbol{q}^{3N}. \tag{36}$$

The observations are very similar to those obtained for the trimer. At very low temperatures the classical calculation tends to the potential minimum. At $T = 1$ K a mean energy of $E = -1216\,\text{cm}^{-1}$ is found. The frozen-Gaussian results are at this temperature already in a very flat regime, in which the mean energy is almost independent of the temperature and approximates the quantum mechanical ground-state energy.

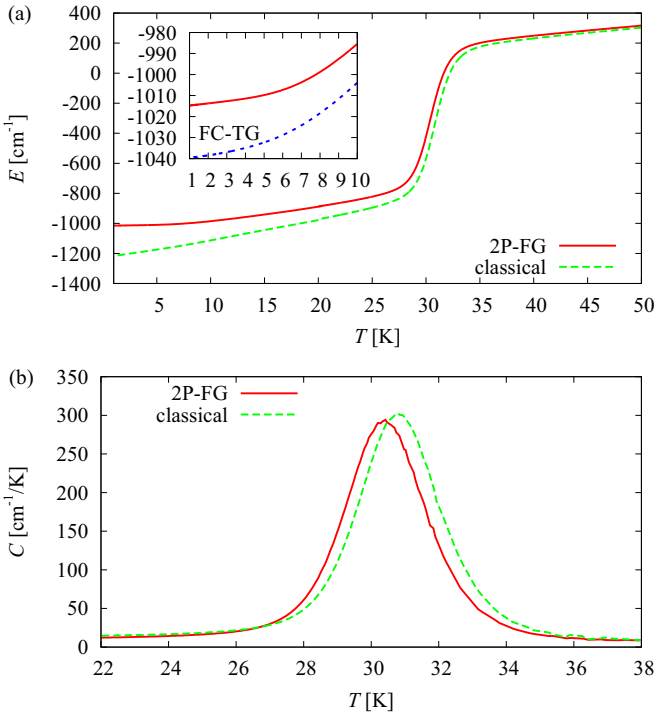

FIG. 1. (Color online) (a) Mean energies of the Ar_6 cluster calculated with the two-parameter frozen-Gaussian propagator (2P-FG) and its classical counterpart. For the high-temperature limit both results agree well. At low temperatures the classical mean energy tends to the potential minimum and the frozen-Gaussian propagator approximates the quantum mechanical ground state. The inset shows a comparison of the 2P-FG method with the fully coupled thawed-Gaussian method (FC-TG). The energies differ by a few percent. (b) Specific heat around the dissociation, which seems to happen in one step.

The method leads to $E_0 \approx -1015\,\text{cm}^{-1}$. In the inset of Fig. 1(a) a comparison with the more flexible fully coupled thawed-Gaussian propagator is shown. It leads to a value of $E_0 \approx -1040\,\text{cm}^{-1}$, i.e., the difference of the ground state's binding energy is only 2.4%. Thus, one may conclude that also for the larger Ar_6 cluster the quality of the frozen-Gaussian propagator is acceptable in comparison with the numerically more expensive thawed-Gaussian variant even for the low-temperature limit.

The dissociation appears in the mean energy as a step. The energy raises almost directly to that of six free particles. This indicates a dissociation of all atoms at once as was observed for the trimer. The same information can be gained from the specific heat, which is shown around the dissociation in Fig. 1(b). One broad peak confirms that the dissociation occurs in one step. The classical calculation shows a transition at a slightly lower temperature, and the difference between the two maxima in the specific heat is approximately 0.5 K, which is lower than for the trimer, where a difference of 1.5 K was observed. Certainly the difference can again be related to the zero point energy in quantum mechanics. This is larger for six atoms than for three and one could expect that also the temperature difference is larger. However, one has to keep in mind that this energy has to be distributed among a larger

number of atoms during the dissociation. Since aside from the small shift in the temperature the dissociation process is almost identical in the classical and the frozen-Gaussian calculation one may conclude that it is a purely classical phenomenon.

E. Structural information for low temperatures and for the dissociation

In addition to the information of the simple derivatives of the partition function the mean distances are studied. Since so far the dissociation seems to be purely classical it is interesting to also compare the structural information with the classical one. To do so, the classical mean distances,

$$\bar{d}_{ij}^{(\mathrm{classical})} = \frac{1}{Z_{\mathrm{cl}}}\left(\frac{\mathrm{k}T}{2\pi\hbar^2}\right)^{3/2N} \int e^{-\beta V(\boldsymbol{q})} |\boldsymbol{q}_i - \boldsymbol{q}_j| \, d\boldsymbol{q}^{3N}, \tag{37}$$

are added in the calculations below.

1. Structure at low temperatures

The mean distances obtained for temperatures below 20 K, i.e., significantly below the dissociation process, are shown in Fig. 2, where first the frozen-Gaussian method (2P-FG) is compared with the classical calculation in Fig. 2(a), and then the fully coupled thawed-Gaussian approximation is added in Fig. 2(b). The most striking observation is that the distances appear in the low-temperature limit in two groups. A group of three "long" distances, of which the values are always above

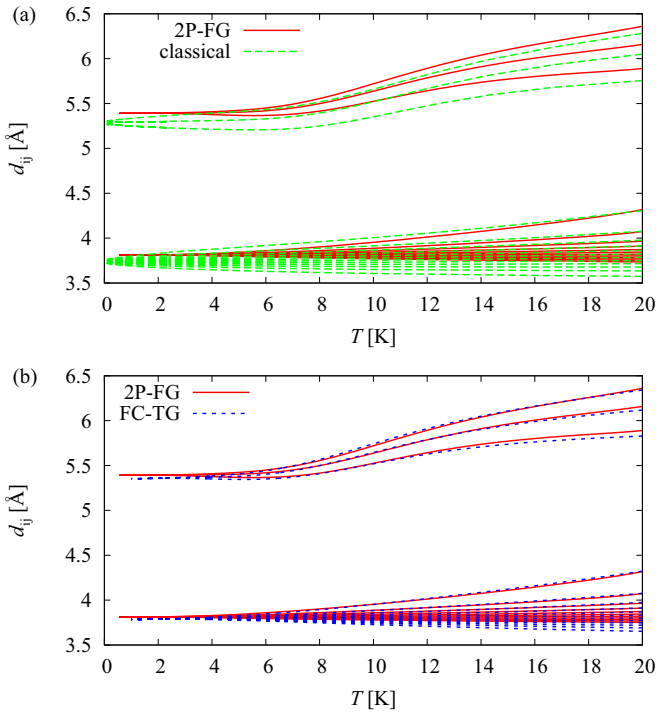

FIG. 2. (Color online) (a) Comparison of the mean values of all 15 distances calculated with the frozen-Gaussian method (2P-FG) and a classical calculation at temperatures $T \leqslant 20$. The distances appear in groups. Three distances converge for $T \to 0$ to values above 5 Å, whereas the remaining 12 are below 4 Å. (b) A comparison of the frozen-Gaussian and thawed-Gaussian method (FC-TG) shows that the mean distances agree very well.

5 Å for $T \to 0$, and a second group of the 12 remaining "short" distances, which converge to a value below 4 Å, exist. This already gives a clear answer to the question about the ground-state configuration of Ar_6. It is consistent with the distances in an octahedron, or in other words, the atoms are located at the centers of the surfaces of its dual polyhedron, viz. the cube. Twelve short distances d_s from the atoms on neighboring surfaces and three longer distances d_l between the atoms on opposite surfaces are expected. The ratio of the distances is supposed to be $d_l = \sqrt{2}d_s$, which is fulfilled excellently in both the classical and semiclassical calculations.

In the classical case the atoms seek directly the potential minima, whereas in the quantum case always a wave function with a finite width leading automatically to larger mean distances is present. Furthermore, in the classical case the fixed octahedron configuration is only observable for $T \to 0$. This is a consequence of the fact that classically every nonvanishing energy allows for a thermal excitation. In contrast to this there should be no excitation possible if $\mathrm{k}T$ is clearly below the energy difference between the ground state and the first excited state in the quantum mechanical case. This is also reflected in the mean distances. For temperatures below $T \approx 3$ K no differences between the distances in one group are observed, and the distances do not change for even lower temperatures. This indicates that the cluster is already in the ground-state configuration.

A comparison of the frozen-Gaussian method with the fully coupled thawed-Gaussian propagator reveals that the distances agree very well. This is in particular true for all larger distances. Also the low-temperature limit shows an excellent agreement. The edge length of the cube containing the octahedron is $d_l = 5.39$ Å in the frozen-Gaussian calculation and $d_l = 5.35$ Å in the thawed-Gaussian approximation. The difference is below 1%, and thus even smaller than that of the mean energy. Obviously the structural information of the frozen-Gaussian method is less affected by the constant Gaussian width approximation.

With the data of Fig. 2 we are also able to estimate the quality of the approximation (17), in which the power series expansion of the distances was introduced. The first-order term retained in the expansion is of the size

$$\frac{\mathrm{Tr}\left(\boldsymbol{\Gamma}_{ii}^{-1} + \boldsymbol{\Gamma}_{jj}^{-1} - \boldsymbol{\Gamma}_{ij}^{-1} - \boldsymbol{\Gamma}_{ji}^{-1}\right)}{6|\boldsymbol{q}_i - \boldsymbol{q}_j|},$$

where for the width matrix (12) $\mathrm{Tr}(\boldsymbol{\Gamma}_{ii}^{-1} + \boldsymbol{\Gamma}_{jj}^{-1} - \boldsymbol{\Gamma}_{ij}^{-1} - \boldsymbol{\Gamma}_{ji}^{-1})/6 = D_2^{-1} = (32\,\text{Å}^{-2})^{-1} = 0.031\,\text{Å}^2$ is obtained. With the knowledge that the typical distances $|\boldsymbol{q}_i - \boldsymbol{q}_j|$ are even in the bound phase of the order of a few Ångströms this correction can be estimated to be always less than 1% of the leading order. Hence, it has at most the same size as the difference between the two semiclassical propagators. Higher orders in the series expansion (17) would lead to even smaller corrections, which do not need to be taken into account since they are below the error of the semiclassical approximation.

2. Dissociation to six free atoms

The distances around the dissociation are shown in Fig. 3, where the classical and 2P-FG results are compared. Since

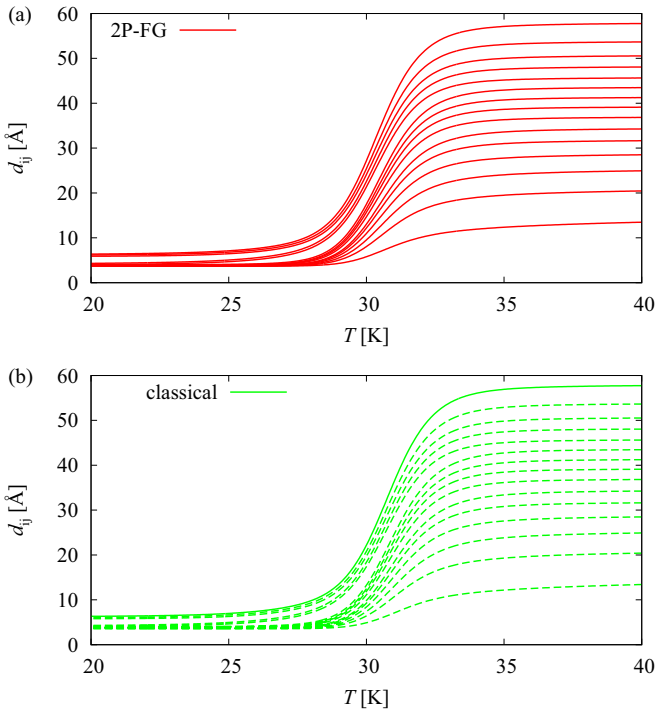

FIG. 3. (Color online) (a) Mean values of all 15 distances calculated with the frozen-Gaussian method (2P-FG) around the dissociation. Two of the smaller distances join the group of the three larger distances starting at $T \approx 23$ K, but then the dissociation occurs at once. (b) The same behavior is observed for the classical calculation.

the frozen-Gaussian approximation is known to provide good results at these temperatures (cf. Ref. [18]), a comparison with the thawed-Gaussian propagator does not give any new information. Figure 3 confirms the finding of the consideration of the mean energy and the specific heat in Fig. 1. The dissociation effect is classical. The semiclassical approximation of the quantum mechanical propagator and the purely classical calculation lead to the same behavior. Apart from a small shift in temperature both diagrams agree very well.

The calculation of the distances gives additional insight into the dissociation process. For temperatures $T \lessapprox 23$ K the groups of short and long distances are unchanged. Above this temperature two of the 12 distances d_s are separating from the others and join the three longer distances d_l. Two new groups with five and 10 distances start to form. For Ar_6 a second isomer in the form of a tri-tetrahedron is known to contribute at increasing temperatures [33]. This would exactly agree with a grouping of five longer and 10 shorter distances and is also visible in Fig. 4, in which the distances of all six atoms from the center of mass are shown for a classical calculation. At low temperatures all distances have almost the same size, which agrees with a pure octahedron configuration. With increasing temperature one distance grows and indicates a coexistence of octahedron and tri-tetrahedron configurations. Signatures of further arrangements of the atoms are not found.

However, this rearrangement of the atoms remains in its beginnings. A new structure cannot completely arise since the whole process does not finish before all distances raise drastically and indicate with this increase the dissociation of

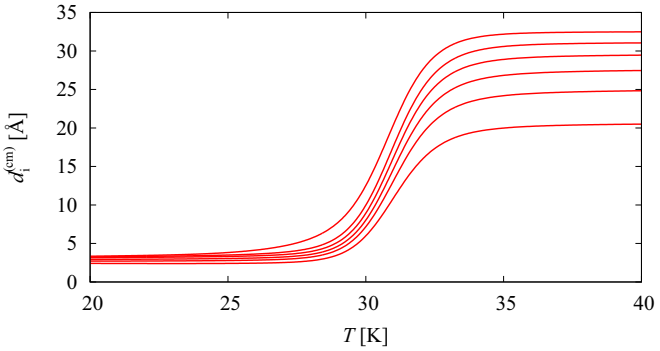

FIG. 4. (Color online) Distances of all six atoms from the center of mass in a classical calculation for $R_c = 35$ Å. Shown is a thermal average of size-ordered distances as explained in Sec. II C. With increasing temperature one distance becomes larger than the others before all raise drastically.

the cluster. Comparisons with calculations, in which due to a smaller value of R_c no dissociation is allowed, show that this effect only appears in connection with the dissociation. Thus, the separation of the two distances is more a precursor of the total destruction of the cluster. The dissociation happens then at once. After the dissociation the distances obtain new almost constant values which correspond to the distribution of atoms moving freely within the confining sphere.

3. Variances of the distances

To learn more about the actual distribution of the distances their standard deviations are shown in Figs. 5(a) and 5(b) for the classical and the 2P-FG method. The most significant feature is the drastic increase of the standard deviations around the transition. At this temperature range parts of the simulated clusters are still in a bound configuration whereas others are already dissociated. The effect is similar and of the same size for the classical and the semiclassical calculation. For temperatures above the dissociation the standard deviations are almost the same for all distances, which is also expected for six free atoms.

Of more interest is the behavior of the standard deviations below the dissociation. The longer distances are expected to show more fluctuations. Additionally two of the shorter distances join the group of the three longer distances for increasing temperatures as a consequence of contributions from two isomers. It can also be expected that these two show higher standard deviations than the short distances since the separation of the two distances does not happen abruptly at one temperature as can be seen in Fig. 3. Consequently, below the dissociation the standard deviations are found to form two groups. One group combines the standard deviations of five distances, i.e., the three longer ones and the two joining them. The other group consists of the standard deviations of the 10 short distances which stay together up to the temperature of the dissociation.

In Figs. 5(a) and 5(b) it seems that the standard deviations always decrease for lower temperatures. This is definitely expected for the classical calculation. The frozen-Gaussian approximation can, since the width of the wave function is determined by the constant values of $\mathbf{\Gamma}$, not reflect the quantum

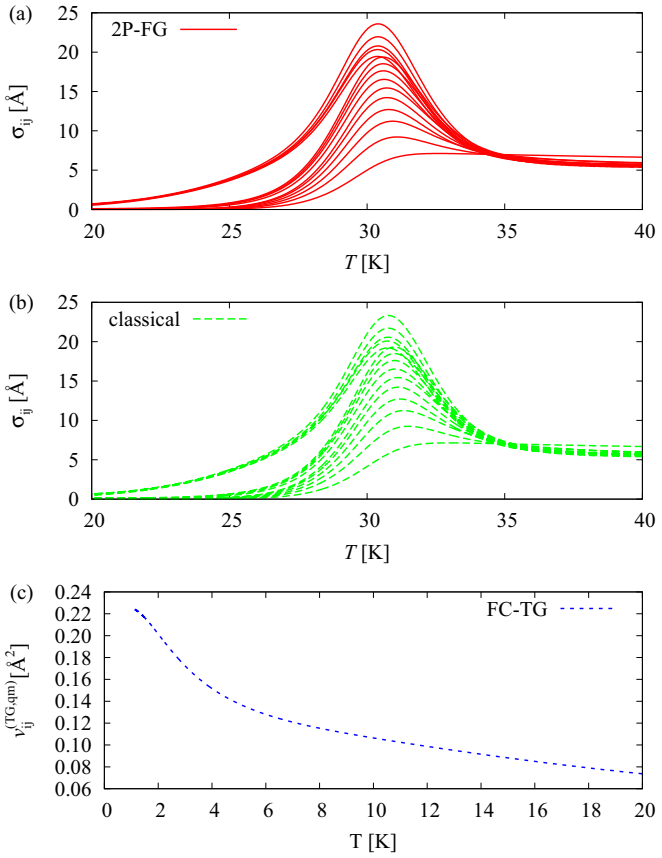

FIG. 5. (Color online) (a) Standard deviations σ_{ij} of the distances in the frozen-Gaussian approximation (2P-FG) and (b) of the classical calculation. They increase drastically around the dissociation. (c) Quantum mechanical part (31) of the variances for the fully coupled thawed-Gaussian propagator. For low temperatures it increases due to an increasing width of the Gaussians.

mechanical expectation that the wave function stretches at lower temperatures. To cover also this effect the quantum mechanical part according to Eq. (31) is plotted in Fig. 5(c). Only the variance of one of the distances is shown since this part is almost identical for all of them in the highly symmetric situation of a monoatomic cluster. At $T \approx 20\,\mathrm{K}$ the variance has approximately the same size as that following from the frozen-Gaussian method $v_{ij}^{(\mathrm{FG,qm})} = \mathrm{Tr}(\mathbf{\Gamma}_{ii}^{-1} + \mathbf{\Gamma}_{jj}^{-1} - \mathbf{\Gamma}_{ij}^{-1} - \mathbf{\Gamma}_{ji}^{-1})/2 = 3D_2^{-1} = 0.093\,\text{Å}^2$. In particular, these quantum mechanical parts of the variances are considerably lower than other contributions in Eqs. (22) and (30). Figure 5(a) would not change with the thawed-Gaussian propagator. Only for temperatures $T \lessapprox 10\,\mathrm{K}$ the extension of the wave function becomes important for a measurement of the distances. For temperatures in the range of the dissociation the information from the frozen-Gaussian method is completely sufficient.

All calculations shown in this section could be implemented and performed easily on a NVIDIA Tesla C2070 GPU. On this architecture a converged result for low temperatures is obtained in less than 20 h. The most critical part is that around the dissociation, where a very detailed sampling for bound configurations has to be done alongside an inclusion of large distances allowing for an unbound cluster. This can require an increase of the sampling points by a factor of 10.

IV. SUMMARY AND OUTLOOK

In this article it was shown that structural information about a cluster of atoms can be obtained with the frozen-Gaussian semiclassical method in a numerically cheap way. The evaluation of the corresponding integrals can be done in parallel to that of the partition function. With this method the full information about all the distances of all combinations of the atoms can be obtained. A comparison with the more flexible thawed-Gaussian propagator revealed that the quality of the distances is on the same level as that of the mean energy or the specific heat, or even better. To avoid inefficient numerical computations of a position space integral an approximation for the distances was introduced. It was possible, however, to show that this approximation does not reduce the quality of the results below that obtained in the semiclassical approximation of the propagator.

On the physical side it was found that with increasing temperatures the Ar_6 cluster undergoes an almost direct transition to six free atoms. However, it shows precursors in the distances. At temperatures slightly below the dissociation a reordering of the atoms starts, in which contributions from a second isomer, viz. a tri-tetrahedron [33], appear, but then vanish in the increasing distances at the dissociation. The dissociation is a purely classical effect. The semiclassical approximation shows exactly the same behavior with just a small shift in the temperature of 0.5 K. Around the dissociation the standard deviations of the distances are almost completely determined by classical contributions. Only for lower temperatures the extension of the wave functions becomes important as was seen in a thawed-Gaussian approximation.

At low temperatures the cluster assumes the shape of an octahedron, where the longer distance between the atoms is $d_l = 5.4\,\text{Å}$, and the shorter has the value $d_s = d_l/\sqrt{2} = 3.8\,\text{Å}$. Classically the fixed configuration is only obtained in the limit $T \to 0$ whereas in the quantum mechanical case the ground-state configuration is present for all temperatures $T \lessapprox 3\,\mathrm{K}$.

The frozen-Gaussian method has proved to provide reliable results for quantum mechanical calculations. There is a large number of investigations which can be done with it. In particular, the results for Ar_3 in [16] and for Ar_6 in this work indicate that the confinement to very small spheres usually applied in the calculation of the partition function and values deduced from it [2–4,41] only sample bound cluster configurations. This is physically realized at high pressures. If one is interested in lower pressures, at which a dissociation is allowed, this is too restrictive to fully understand the low-temperature behavior of the clusters. The dissociation can set in before structural changes or a melting can be observed. To take this into account it is necessary to advance the investigations done here to clusters with higher numbers of atoms. In particular, the cases of Ar_{13} [42–44], Ne_{13} [3] or Ne_{38} [4] are of special interest since they showed interesting structural transformations in the nondissociated cases. Whereas the stronger quantum effects in the completely bound case are well covered by a variable width matrix the numerically cheaper frozen-Gaussian method has advantages in the numerically more challenging case of

the dissociation requiring a sampling of bound and unbound configurations of the atoms. The exactness of both methods can then be monitored and (if necessary) improved with the series expansion of the imaginary-time propagator [18,34,35].

The importance of the series expansion is not restricted to the dissociation. Most effects in rare gas clusters such as structural transformations or dissociations appear at such low temperatures that it is necessary to analyze whether the semiclassical approximations used in the calculations correctly reproduce the true quantum mechanical behavior. An important example will be Ne_{38}, for which strong differences are found between the approximate quantum computations and a purely classical theory [6].

ACKNOWLEDGMENTS

H.C. is grateful for a Minerva fellowship. He thanks Eli Pollak for valuable comments and kind hospitality at the Weizmann Institute of Science, where this work was started.

[1] J. P. Neirotti, D. L. Freeman, and J. D. Doll, J. Chem. Phys. **112**, 3990 (2000).
[2] C. Predescu, D. Sabo, J. D. Doll, and D. L. Freeman, J. Chem. Phys. **119**, 12119 (2003).
[3] P. A. Frantsuzov and V. A. Mandelshtam, J. Chem. Phys. **121**, 9247 (2004).
[4] C. Predescu, P. A. Frantsuzov, and V. A. Mandelshtam, J. Chem. Phys. **122**, 154305 (2005).
[5] R. P. White, S. M. Cleary, and H. R. Mayne, J. Chem. Phys. **123**, 094505 (2005).
[6] P. A. Frantsuzov, D. Meluzzi, and V. A. Mandelshtam, Phys. Rev. Lett. **96**, 113401 (2006).
[7] R. Pérez de Tudela, M. Márquez-Mijares, T. González-Lezana, O. Roncero, S. Miret-Artés, G. Delgado-Barrio, and P. Villarreal, J. Chem. Phys. **132**, 244303 (2010).
[8] G. Adjanor, M. Athènes, and F. Calvo, Eur. Phys. J. B **53**, 47 (2006).
[9] E. Pahl, F. Calvo, L. Koči, and P. Schwerdtfeger, Angew. Chem. Int. Ed. **47**, 8207 (2008).
[10] I. Georgescu and V. A. Mandelshtam, J. Chem. Phys. **135**, 154106 (2011).
[11] I. Georgescu and V. A. Mandelshtam, J. Chem. Phys. **137**, 144106 (2012).
[12] B. J. Berne and D. Thirumalai, Annu. Rev. Phys. Chem. **37**, 401 (1986).
[13] N. Makri, Annu. Rev. Phys. Chem. **50**, 167 (1999).
[14] D. M. Ceperley, AIP Conf. Proc. **690**, 85 (2003).
[15] D. D. Frantz, D. L. Freeman, and J. D. Doll, J. Chem. Phys. **97**, 5713 (1992).
[16] H. Cartarius and E. Pollak, J. Chem. Phys. **134**, 044107 (2011).
[17] J. Liu and W. H. Miller, J. Chem. Phys. **134**, 104102 (2011).
[18] H. Cartarius and E. Pollak, Chem. Phys. **399**, 135 (2012).
[19] M. Kryvohuz, Chem. Phys. **407**, 124 (2012).
[20] R. Conte and E. Pollak, J. Chem. Phys. **136**, 094101 (2012).
[21] R. D. Etters and J. Kaelberer, Phys. Rev. A **11**, 1068 (1975).
[22] D. M. Leitner, R. S. Berry, and R. M. Whitnell, J. Chem. Phys. **91**, 3470 (1989).
[23] D. M. Leitner, J. D. Doll, and R. M. Whitnell, J. Chem. Phys. **94**, 6644 (1991).
[24] P. V. Elyutin, V. I. Baranov, E. D. Belega, and D. N. Trubnikov, J. Chem. Phys. **100**, 3843 (1994).
[25] T. González-Lezana, J. Rubayo-Soneira, S. Miret-Artés, F. A. Gianturco, G. Delgado-Barrio, and P. Villarreal, J. Chem. Phys. **110**, 9000 (1999).
[26] P. Svrčková, A. Vítek, F. Karlický, I. Paidarová, and R. Kalus, J. Chem. Phys. **134**, 224310 (2011).
[27] F. Blanco and G. García, J. Phys.: Conf. Ser. **438**, 012012 (2013).
[28] W. Unn-Toc, N. Halberstadt, C. Meier, and M. Mella, J. Chem. Phys. **137**, 014304 (2012).
[29] M. Mella, J. Chem. Phys. **131**, 124309 (2009).
[30] F. Calvo, F. Naumkin, and D. Wales, Chem. Phys. Lett. **551**, 38 (2012).
[31] I. Mähr, F. Zappa, S. Denifl, D. Kubala, O. Echt, T. D. Märk, and P. Scheier, Phys. Rev. Lett. **98**, 023401 (2007).
[32] F. Calvo and P. Parneix, J. Phys. Chem. A **113**, 14352 (2009).
[33] G. Franke, E. R. Hilf, and P. Borrmann, J. Chem. Phys. **98**, 3496 (1993).
[34] J. Shao and E. Pollak, J. Chem. Phys. **125**, 133502 (2006).
[35] D. H. Zhang, J. Shao, and E. Pollak, J. Chem. Phys. **131**, 044116 (2009).
[36] K. Kwon and A. Moscowitz, Phys. Rev. Lett. **77**, 1238 (1996).
[37] B. Ulrich, A. Vredenborg, A. Malakzadeh, L. P. H. Schmidt, T. Havermeier, M. Meckel, K. Cole, M. Smolarski, Z. Chang, T. Jahnke, and R. Dörner, J. Phys. Chem. A **115**, 6936 (2011).
[38] R. Conte and E. Pollak, Phys. Rev. E **81**, 036704 (2010).
[39] P. Frantsuzov, A. Neumaier, and V. A. Mandelshtam, Chem. Phys. Lett. **381**, 117 (2003).
[40] R. A. Aziz and M. J. Slaman, Mol. Phys. **58**, 679 (1985).
[41] P. A. Frantsuzov and V. A. Mandelshtam, J. Chem. Phys. **128**, 094304 (2008).
[42] G. Franke, E. Hilf, and L. Polley, Z. Phys. D **9**, 343 (1988).
[43] P. Borrmann, Comput. Mater. Sci. **2**, 593 (1994).
[44] C. J. Tsai and K. D. Jordan, J. Chem. Phys. **99**, 6957 (1993).